MOLECULAR AND CELLULAR BIOLOGY, Feb. 2003, p. 1163–1174 Vol. 23, No. 4
0270-7306/03/$08.00+0 DOI: 10.1128/MCB.23.4.1163–1174.2003

Small Maf Compound Mutants Display Central Nervous System Neuronal Degeneration, Aberrant Transcription, and Bach Protein Mislocalization Coincident with Myoclonus and Abnormal Startle Response

Fumiki Katsuoka,[1,2] Hozumi Motohashi,[1,2] Yuna Tamagawa,[1] Shigeo Kure,[3] Kazuhiko Igarashi,[4] James Douglas Engel,[2]* and Masayuki Yamamoto[1]*

Institute of Basic Medical Sciences and Center for Tsukuba Advanced Research Alliance, University of Tsukuba, Tsukuba 305-8577,[1] Department of Medical Genetics, Tohoku University School of Medicine, Sendai 980-8574,[3] and Department of Biomedical Chemistry, Graduate School of Biomedical Sciences, Hiroshima University, Hiroshima 734-8551,[4] Japan, and Department of Cell and Developmental Biology and Center for Organogenesis, University of Michigan, Ann Arbor, Michigan 48109-0616[2]

Received 5 August 2002/Returned for modification 24 September 2002/Accepted 7 November 2002

The small Maf proteins form heterodimers with CNC and Bach family proteins to elicit transcriptional responses from Maf recognition elements (MAREs). We previously reported germ line-targeted deficiencies in *mafG* plus *mafK* compound mutant mice. The most prominent mutant phenotype was a progressive *maf* dosage-dependent neuromuscular dysfunction. However, there has been no previous report regarding the effects of altered small-*maf* gene expression on neurological dysfunction. We show here that MafG and MafK are expressed in discrete central nervous system (CNS) neurons and that *mafG*::*mafK* compound mutants display neuronal degeneration coincident with surprisingly selective MARE-dependent transcriptional abnormalities. The CNS morphological changes are concurrent with the onset of a neurological disorder in the mutants, and the behavioral changes are accompanied by reduced glycine receptor subunit accumulation. Bach/small Maf heterodimers, which normally generate transcriptional repressors, were significantly underrepresented in nuclear extracts prepared from *maf* mutant brains, and Bach proteins fail to accumulate normally in nuclei. Thus compound *mafG*::*mafK* mutants develop age- and *maf* gene dosage-dependent cell-autonomous neuronal deficiencies that lead to profound neurological defects.

The small Maf proteins were originally identified by their strong homology to the transforming v-Maf oncoprotein of avian retrovirus AS42 (16). Three members constitute the small Maf family, MafF, MafG, and MafK, but no differences between them have been revealed in functional studies (14). All three small Maf proteins possess a basic region-leucine zipper (bZip) motif that mediates DNA binding and dimer formation; however, they lack any recognizable transcriptional effector domain. The small Maf proteins can form homodimers or heterodimers among themselves, and they can also heterodimerize with other bZip transcription factors, including CNC proteins, Bach proteins, and Fos family members, and thus can bind to Maf recognition elements (MAREs) in DNA (24, 25). Large Maf proteins and AP-1 family members also bind to MAREs, as the extended MARE sequence also contains an internal tetradecanoyl phorbol acetate-responsive element (24, 25). All of these factors have the potential to participate in transcriptional regulation through MAREs in the promoters and enhancers of many different genes, most prominently in the hematopoietic system but also in key phase II detoxifying-enzyme genes (11, 24).

One powerful approach to glean insight into the functional roles of specific gene products is through loss-of-function analysis. To date, three of the four *CNC* genes have been disrupted by gene targeting, and conspicuous phenotypes have been reported. For example, *p45 NF-E2*-null mutant mice are severely thrombocytopenic and therefore defective in megakaryopoiesis and platelet production (33). *nrf1*-null mutant mice die during gestation of a non-cell-autonomous anemia (5). *nrf2*-null mutant mice are viable but have severely impaired antioxidant and phase II detoxification enzyme gene responses (11).

The small Maf proteins are obligatory partner molecules of CNC and Bach family proteins in generating both repressing and activating transcriptional activities. The small Maf proteins are expressed in broadly overlapping, but individually distinct, patterns (27), and their expression changes dynamically during embryonic development (9, 15, 22). These observations suggested that small Maf abundance in any given tissue could be critical for MARE-dependent gene regulation. However, no apparent phenotype was detected in either *mafK*- or *mafF*-null mutant mice (19, 27, 31). In contrast, *mafG* mutant mice displayed both mild neurological and hematological phenotypes (31). Because of their partially overlapping embryonic expression profiles and apparently identical biochemical characteristics, we suspected that the small Maf proteins might be par-

* Corresponding author. Mailing address for James Douglas Engel: Department of Cell and Developmental Biology and Center for Organogenesis, University of Michigan Medical School, Ann Arbor, MI 48109-0616. Phone: (734) 615-7509. Fax: (734) 763-1166. E-mail: engel@umich.edu. Mailing address for Masayuki Yamamoto: Institute of Basic Medical Sciences and Center for Tsukuba Advanced Research Alliance, University of Tsukuba, Tsukuba 305-8577, Japan. Phone: 81-298-53-6158. Fax: 81-298-53-7318. E-mail: masi@tara.tsukuba.ac.jp.

tially or completely redundant for any single disruption in gene function.

After combining the *maf* mutations, we discovered that the *mafG*::*mafK* compound mutants displayed far more severe phenotypes than did mutants with the *mafG* mutation alone: thrombocytopenia was exacerbated (thus phenocopying the *p45 NF-E2* mutation) (33), while the neurological phenotype presented much earlier in development (28). Only a fraction of *mafG*$^{-/-}$ mutant mice displayed hind leg clasping, a mild motor dysfunction, with initial onset at about 6 months of age (31). In contrast, *mafG*$^{-/-}$::*mafK*$^{+/-}$ (bearing one active *mafK* allele) mice displayed a more severe neuromuscular disorder, with a far earlier onset in all of the mice. Neither *mafG*$^{+/-}$::*mafK*$^{+/-}$ nor *mafG*$^{+/-}$::*mafK*$^{-/-}$ mice displayed a significant phenotype (28). Therefore, based on the severity of these phenotypes, the genotypes of the compound *maf* mutant mice could be ordered by rank: rank 1 (essentially unaffected mice), *mafK*$^{-/-}$, *mafG*$^{+/-}$::*mafK*$^{+/-}$, and *mafG*$^{+/-}$::*mafK*$^{-/-}$; rank 2 (mice with mild adult onset), *mafG*$^{-/-}$; rank 3 (mice with severe pubertal onset), *mafG*$^{-/-}$::*mafK*$^{+/-}$; rank 4 (mice that died at weaning), *mafG*$^{-/-}$::*mafK*$^{-/-}$. When we analyzed the expression of all three small *maf* genes in a spectrum of different tissues by RNase protection and quantitative PCR, we found that nearly 90% of total small *maf* mRNA expressed in the brain was derived from *mafG* (28). Consequently, the phenotypic severity is what might have been predicted from the small Maf expression abundances. These results implied that gene dosage (and thus the total small Maf concentration) might be an important underlying cause of the neurological disorder and thus that small Maf proteins might act upstream in a motor pathway that normally regulates an unknown, but critical, behavioral determinant(s).

In support of this "Maf dosage" hypothesis, we recently reported that small-Maf protein abundance is crucial for MARE-dependent regulation of the terminal stages of megakaryopoiesis (23). However, since the *mafG* mutants, but not any *CNC* gene mutants, additionally exhibited a neurological phenotype, we exploited this unique, dosage-dependent characteristic of the small *maf* gene loss-of-function mutations to explore the molecular mechanisms underlying the neurological disorder.

We first examined tissues histologically to identify changes in neural tissue(s) that correlated with the progressive motor disease. We found that pathological changes initiated after birth and were widespread in neurons of the central nervous system (CNS) but not in glial cells. The *maf* mutant mice displayed a hypertonic motor disorder and abnormal responses to startle stimuli. In exploring similarities between the *maf* mutants and mice with spontaneous neurological mutations that have been reported in the literature, we discovered that mice bearing mutant glycine receptors also exhibited abnormal startle responses (17, 18, 30). In keeping with the hypothesis that the pathways leading to the similar phenotypes might intersect, we found that the abundance of the glycine receptor α 1 (Glra1) subunit is reduced in symptomatic *maf* mutant mice and that the progression of neurological changes in the *maf* mutants begins postnatally at 3 weeks, coincident temporally with *Glra1* gene transcriptional induction in wild-type mice. Although we anticipated that antioxidant genes in the CNS that are normally regulated through MAREs would be repressed in the mutants, we observed instead only selective induction of MARE-dependent antioxidant genes. We found that CNS MARE-binding proteins, comprising in part Bach/small Maf heterodimers, were diminished in symptomatic mutant animals and that nuclear accumulation of the Bach proteins was severely impaired. We conclude from these data that compound *mafG*$^{-/-}$::*mafK*$^{+/-}$ mutant mice display cell-autonomous neuronal abnormalities that are accompanied by misregulated neuronal MARE-binding activity and that one element of the complex neuropathology exhibited by these mice may be due to a glycine receptor deficiency. Thus the small Maf proteins play a critical role in the maintenance of normal CNS function, as they do in megakaryopoiesis.

MATERIALS AND METHODS

Behavioral studies. A cohort of 31 *mafG*$^{+/-}$::*mafK*$^{+/-}$ mice and 30 *mafG*$^{-/-}$::*mafK*$^{+/-}$ mice were tested at 3, 6, and 9 weeks of age to determine the time of onset and penetrance of the neurological phenotype. When a mouse was held by the tail and displayed hind limb clasping (see Fig. 1A) within 1 min, it was scored as positive. When a mouse was put on the table and myoclonus was triggered in limb extremities at least once within a minute, this mouse was judged to display myoclonus.

Eight- to 11-week-old mice were used for testing acoustic responses. The MRC Institution of Hearing Research click box generates a brief 18- to 20-kHz tone at 94 dB sound pressure level. For measuring locomotor activity, an empty plastic cage was used and locomotion was recorded by SUPERMEX (Muromachi Kikai Co.). Ambulation was scored by using a personal computer interfaced to a mouse body temperature-sensitive sensor (6, 20). To evaluate diminished locomotor activity after acoustic stimuli, we adopted the value of the mean locomotor activity for 2 min after a stimulus divided by the activity for the 5 min preceding the stimulus. Five mice of each genotype were tested, and acoustic stimuli were generated sequentially three times, separated by 10-min intervals.

LacZ activity. Mouse brains were fixed in 1% formaldehyde–0.2% glutaraldehyde–0.02% NP-40 in phosphate-buffered saline and embedded in OCT compound (Tissue-Tek; Sakura). Sections were stained with X-Gal (5-bromo-4-chloro-3-indolyl-β-D-galactopyranoside) solution as previously described (15). Nuclear fast red was used for counterstaining.

Histological analyses. Mouse tissues were fixed in 3.7% formaldehyde and embedded in paraffin. For Nissl staining, the paraffin was removed prior to cresyl violet staining. For ubiquitin immunostaining, sections were processed for immunohistochemistry with the ABC horseradish peroxidase kit (Vector Laboratory) after paraffin removal. The ubiquitin antibody (Santa Cruz Biotechnology) was diluted to 1:200, diaminobenzidine was used as the substrate for chromogen development, and methyl green was used for counterstaining.

In situ hybridization. Mouse brain stems were fixed in 4% paraformaldehyde-phosphate-buffered saline and embedded in paraffin. In situ hybridizations were carried out with a digoxigenin-alkaline phosphatase system (Roche). The *HO-1* cDNA in pBluescript was a generous gift from T. Ishii (University of Tsukuba) and was used to generate RNA probes. Hybridization was performed as previously described (22).

RNA blots. Total RNA was prepared by using Isogen (Nippon Gene). RNA was electrophoresed on a formaldehyde-agarose gel and transferred to a nylon membrane. ^{32}P-labeled probes were prepared from the same *HO-1* cDNA that was used for in situ hybridization, *Glra1* and *Glrb* cDNAs were generated by PCR, and NMDAR1 was a generous gift from S. Nakanishi (Kyoto University).

Electrophoretic mobility shift assay (EMSA). Brain nuclear extracts were prepared as described previously (4). Double-stranded MARE oligonucleotide probe no. 25 (14) was radiolabeled with ^{32}P, and incubation of the probe and nuclear extracts was carried out as described previously (14). The protein-DNA complexes and free probe were resolved by electrophoresis on a 5% polyacrylamide gel in 1× Tris-borate-EDTA buffer. An anti-Bach antibody (F69-1 [29]) and an anti-small Maf antibody (8) were used as originally described.

Western blots. For the detection of Bach proteins, 10 μg of nuclear extract or whole-cell extract was separated by sodium dodecyl sulfate-polyacrylamide gel electrophoresis and then transferred to a polyvinylidene difluoride membrane. Expression of Bach and Nrf1 proteins was examined with the anti-pan-Bach antibody (F69-1) and an anti-Nrf1 antibody (Santa Cruz Biotechnology), respectively. For the detection of the Glra1 subunit, whole-cell extracts were prepared from brain stems of 7-month-old mice. Thirty micrograms of protein was used

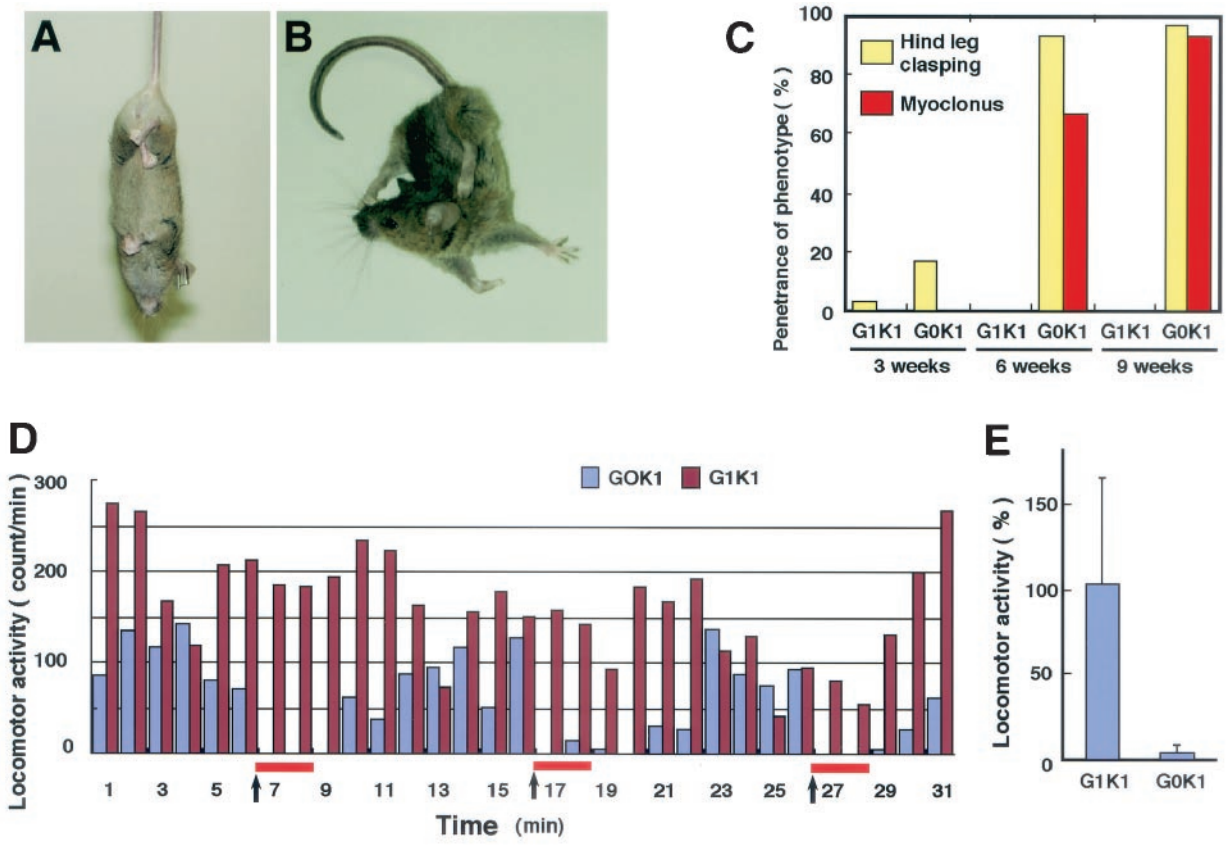

FIG. 1. Behavioral analysis of *mafG*::*mafK* compound mutant mice. (A) A $mafG^{-/-}$::$mafK^{+/-}$ mutant mouse (6 weeks old) displaying characteristic hind leg clasping. (B) A $mafG^{-/-}$::$mafK^{+/-}$ mutant mouse (10 weeks) with long-lasting myoclonus. (C) The penetrance of the motor disorder was examined at 3, 6, and 9 weeks of age. Bars indicate frequencies of mice displaying each phenotype. G1K1 and G0K1, $mafG^{+/-}$::$mafK^{+/-}$ control and $mafG^{-/-}$::$mafK^{+/-}$ mutant, respectively. (D) Representative pattern of locomotor activities of $mafG^{-/-}$::$mafK^{+/-}$ (mutant) and $mafG^{+/-}$::$mafK^{+/-}$ (control) mice. Each bar indicates the frequency of ambulation per minute. Arrows, times of acoustic stimuli. (E) Comparison of the influences of acoustic stimuli on the locomotor activities of mutant and control mice. The mean ambulation count for 2 min after stimulus (red bars in panel D) was divided by that for 5 min before stimulus. This value was averaged for five independent animals and depicted as a bar. Error bars, standard deviations.

per sample lane. The antibody recognizing the Glra1 subunit was purchased from Calbiochem.

Transfection and immunostaining. pCMV/Bach1 and pCMV/Bach2 were used for forced expression of Bach1 and Bach2, respectively (29). pIM-MafK and pIM-MafKL2PM4P were used for transient expression of MafK and a MafK leucine zipper-defective mutant (MafKL2PM4P), respectively (23). These expression vectors were transfected into NIH 3T3 cells with FuGENE6 (Roche). At 24 h after transfection, cells were fixed with methanol at −20°C for 5 min and treated with 0.1% Triton X-100. After being blocked with 2% goat serum, cells were reacted with the anti-Bach1 antibody for 1 h and then with fluorescein isothiocyanate-conjugated anti-rabbit immunoglobulin G. After the secondary-antibody solution was washed away, cell nuclei were stained with DAPI (4′,6′-diamidino-2-phenylindole). One hundred transfected cells were examined and classified into three categories: C>N (predominantly cytoplasmic staining); C=N (a roughly equal distribution between cytoplasmic and nuclear compartments), and C<N (predominantly nuclear staining).

RESULTS

$mafG^{-/-}$::$mafK^{+/-}$ mice display a progressive motor disorder. The neurological phenotype in *mafG* null mutant mice was detectable only after approximately 6 months of age and was incompletely penetrant (31). The same (but fully penetrant) phenotype appeared earliest in $mafG^{-/-}$::$mafK^{-/-}$ (compound null) mutant mice, but these animals survived only to about 3 weeks of age (28). We therefore chose to subject $mafG^{-/-}$::$mafK^{+/-}$ compound mutants, bearing one active *mafK* allele, to detailed scrutiny since they had an almost normal life span and yet the neurological phenotype occurred early and was fully penetrant. For this analysis we compared the neurological phenotypes of the $mafG^{-/-}$::$mafK^{+/-}$ mice to those of the $mafG^{+/-}$::$mafK^{+/-}$ control littermates (mutant for one allele of both *mafK* and *mafG*), which display no neurological phenotype.

More than one-half of the $mafG^{-/-}$::$mafK^{+/-}$ mutant mice developed a characteristic hind leg clasping by the sixth week after birth (Fig. 1A and C). Two-thirds of the mutant mice began to show intermittent and long-lasting hind limb or tetrapodic myoclonus (Fig. 1B), and this aberrant behavior was fully penetrant by 9 weeks of age (Fig. 1C). None of the $mafG^{+/-}$::$mafK^{+/-}$ (Fig. 1C) control mice were affected.

Myoclonus occurred spontaneously in the mutant mice but could also be triggered by external stimuli. By monitoring the nocturnal behavior of the mutant mice, we discovered that the hind leg myoclonus was triggered when the mutant mice began to eat with their forepaws. Myoclonus was also observed when

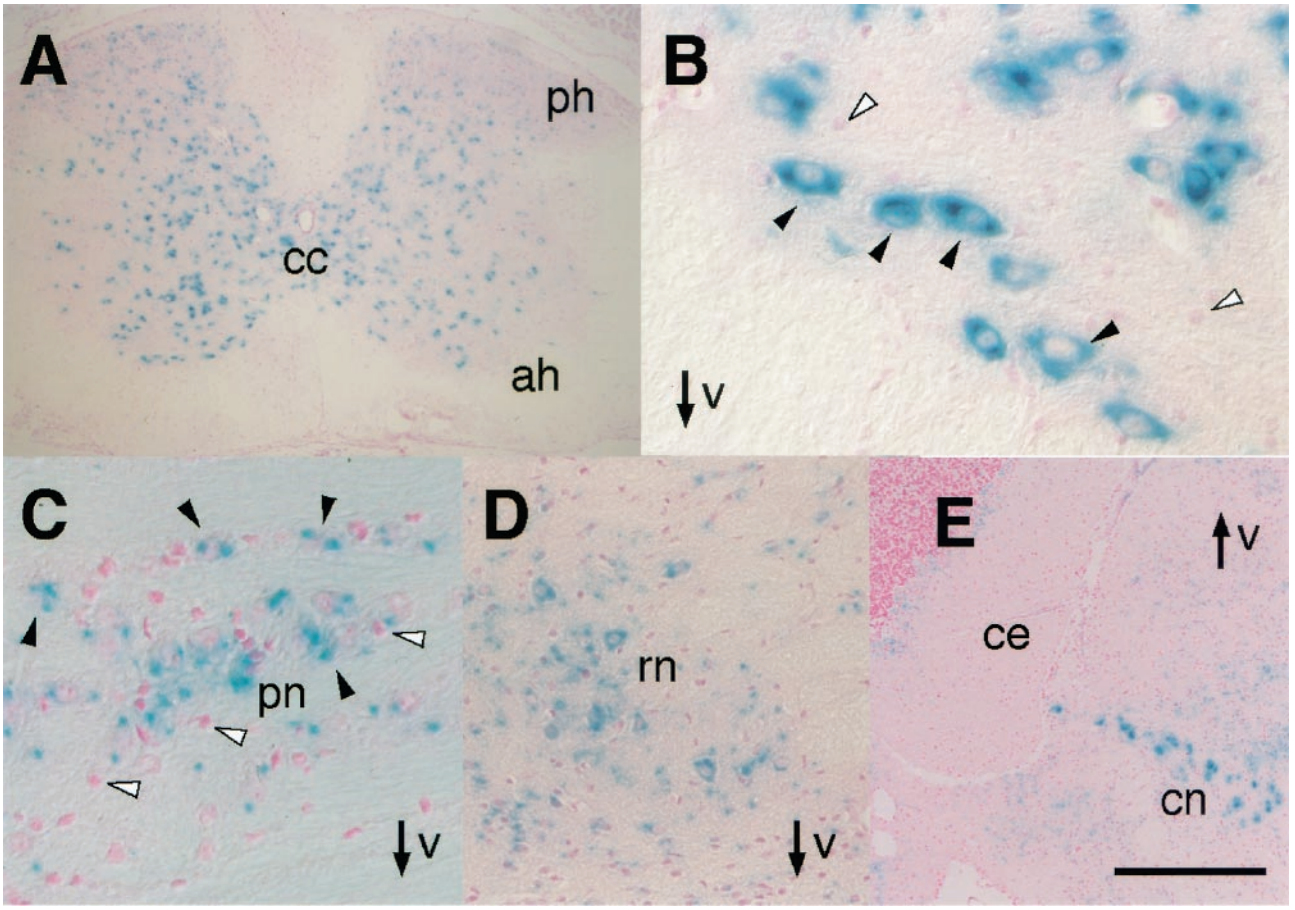

FIG. 2. *mafG* gene expression in the CNS. Tissue sections from a *mafG*$^{+/-}$ mouse were prepared and stained for β-galactosidase activity. LacZ activity (blue) was observed exclusively in neurons (not in glial cells) in the spinal cord (A and B), pons (C), medulla (D), and cerebellar nuclei (E). Solid arrowheads, neurons; open arrowheads, glia; arrows beside V, ventral side. Scale bar, 450 (A and E), 90 (B), 110 (C), or 150 μm (D). cc, central canal; ah, anterior horn; ph, posterior horn; pn, pontine nuclei; rn, reticular nuclei; cn, cerebellar nuclei; ce, cerebellum.

the mutants approached the edge of a table during free locomotion, behavior that seemed to be triggered by visual stimuli (data not shown).

Anticipating that this neurological deficiency might originate in the CNS (see below), we monitored the locomotor activity of *mafG*$^{-/-}$::*mafK*$^{+/-}$ mutant mice in response to acoustic stimuli, and Fig. 1D shows a representative pattern of activity before and after stimulation. The activity of *mafG*$^{-/-}$::*mafK*$^{+/-}$ mutant mice was quantifiably repressed after stimulation, while *mafG*$^{+/-}$::*mafK*$^{+/-}$ control littermates displayed little response. Five mice of each genotype were examined, and the average locomotor activities for 2 min following the acoustic stimulus were compared. The data depict a qualitative difference in acoustic response between *mafG*$^{+/-}$::*mafK*$^{+/-}$ control and *mafG*$^{-/-}$::*mafK*$^{+/-}$ mutant mice (Fig. 1E).

MafG and MafK are both expressed in neurons. We previously reported that MafK is widely expressed in neurons, but not in glial cells, of the CNS. The large cells morphologically identified as neurons generally express MafK mRNA in the spinal cord, brain stem, hippocampus, and dorsal root ganglia (22). To ask whether diminished MafK and MafG expression might lead to exclusively neuronal deficiencies, we examined *mafG* expression in the CNS by monitoring the expression of the *lacZ* gene, which was used to replace the coding sequences of *mafG* during the generation of the targeted mutant mice (31). β-Galactosidase activity was observed primarily in neurons, but not in glia, of the spinal cord (Fig. 2A and B); this was also true in the brain stem (Fig. 2C to E) and hippocampus and dorsal root ganglia (data not shown). Especially in spinal cord gray matter and cerebellar nuclei, almost all the recognizable neurons expressed MafG (Fig. 2A and E) as well as MafK (22), indicating overlapping expression of the two genes. The data show that MafG and MafK are predominantly, if not exclusively, expressed in neurons in the CNS.

CNS neuronal degeneration in *mafG*$^{-/-}$::*mafK*$^{+/-}$ mice. To investigate the underlying cellular basis for the observed neuronal disorder, we performed histological examination of neural tissues from 10-week-old *mafG*$^{-/-}$::*mafK*$^{+/-}$ mice that displayed pathological behavior. The numbers of Nissl-staining neurons in the gray matter of the spinal cord in *mafG*$^{-/-}$::*mafK*$^{+/-}$ mutant mice and *mafG*$^{+/-}$::*mafK*$^{+/-}$ controls appeared to be almost the same, albeit with slightly weaker staining in the mutants (Fig. 3A and B). When the same sections were examined at higher magnification, however, a conspicuous difference between the two genotypes was consistently observed. Many of the neuronal nuclei in the affected mouse

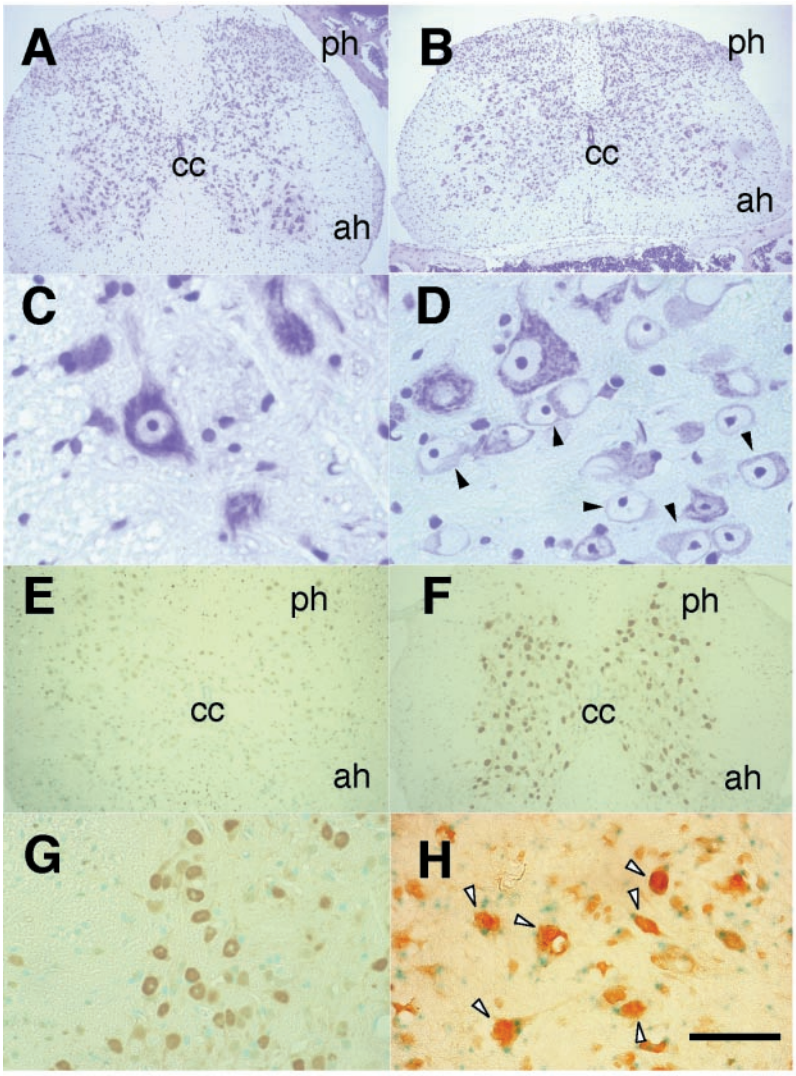

FIG. 3. Histopathological changes in CNS neurons of *maf* mutant mice. (A to D) Nissl staining of spinal cord sections from 10-week-old *mafG*$^{+/-}$::*mafK*$^{+/-}$ control mice (A and C) and *mafG*$^{-/-}$::*mafK*$^{+/-}$ mutant mice (B and D) displaying myoclonus. Solid arrowheads (D), swollen nuclei with minimal cytoplasm in the affected mice. (E to G) Immunostaining for ubiquitin in spinal cord sections from control *mafG*$^{+/-}$::*mafK*$^{+/-}$ mice (E) and *mafG*$^{-/-}$::*mafK*$^{+/-}$ mutant mice (F and G). The mutants display far more intense staining, primarily in neuronal nuclei (G). (H) Double staining for β-galactosidase activity and ubiquitin immunohistological activity on brain stem sections prepared from 4-week-old *mafG*$^{-/-}$::*mafK*$^{+/-}$ mutant mice. Note that all the cells in which ubiquitin has accumulated (intense brown signal) are also LacZ positive (open arrowheads). Scale bar, 400 (A, B, E, and F), 40 (C and D), 120 (G), or 60 μm (H). Abbreviations are as defined in the legend to Fig. 2.

spinal cord were swollen, and their cytoplasm was thin, containing few Nissl bodies (Fig. 3C and D). The neurons in the anterolateral column of the spinal cord were less severely affected but still contained fewer Nissl bodies than controls. The same morphological characteristics were observed along the entire length of the spinal cord and brain stem. Similarly affected neurons were also distributed throughout the thalamus, hippocampus, and cerebral cortex (data not shown). These same cellular changes were not detected in the comparable tissues of 1-week-old mutants but became apparent even as early as 3 weeks of age (before the mutant mice became symptomatic; Fig. 1C). These results suggested that the abnormal neurons in these young *mafG*$^{-/-}$::*mafK*$^{+/-}$ mutant mice could be degenerating.

One of the most prominent histological features of many neurodegenerative disorders is the intracellular deposition of aggregated, ubiquitinated proteins (1). Since many neurons with swollen nuclei were observed in the symptomatic mice, we suspected that protein aggregates might have accumulated in their nuclei, and therefore we assessed these cells for evidence of ubiquitinated proteins. Indeed, spinal cord neurons of asymptomatic 3-week old *mafG*$^{-/-}$::*mafK*$^{+/-}$ mutant mice showed greatly elevated spinal cord ubiquitin immunostaining compared to those of their control littermates (Fig. 3F and E, respectively), primarily in the nuclei of the affected neurons (Fig. 3G). Ubiquitin immunostaining was also observed in the brain stem, thalamus, hippocampus, and subsections of the cerebral cortex of the mutants (data not shown).

Importantly, the distribution of the affected neurons in mutant mice that were identified by Nissl staining largely over-

lapped that of ubiquitin-positive cells. In contrast, no ubiquitin immunostaining was observed in Purkinje cells or granule cells of the cerebellum (data not shown). An increased high-molecular-weight smear of ubiquitin immunoreactivity was observed in whole-cell lysates prepared from *mafG*$^{-/-}$::*mafK*$^{+/-}$ mutant spinal cords in comparison to controls (data not shown). Thus the increased neuronal nuclear ubiquitin immunostaining in the mutant mice reflected coordinately increased accumulation of ubiquitinated protein aggregates in the same cells. Elevated ubiquitin levels were not detected in spinal cords of 1-week-old mutant mice, further supporting the hypothesis that pathological changes in these neurons are initially detectable around 3 weeks of age, coincident with the earliest onset of any nervous system phenotype (Fig. 1C).

A comparison between the expression profiles of MafK (22) and MafG (Fig. 2) taken together with the results of ubiquitin immunostaining suggested that the neurodegeneration was a cell-autonomous phenomenon. To substantiate this possibility, we performed double staining for both ubiquitin (using immunohistochemistry) and β-galactosidase (monitoring LacZ activity from the *mafG* knock-in) on sections from the spinal cords of 4-week-old *mafG*$^{-/-}$::*mafK*$^{+/-}$ mice. As shown Fig. 3H, almost all of the ubiquitin-positive cells also stained for LacZ activity. Taken together, these results strongly suggest that the neurodegeneration observed in the *mafG*$^{-/-}$::*mafK*$^{+/-}$ mice is cell autonomous.

Accumulation of ubiquitin conjugates suggested that the molecular mechanisms responsible for the neuronal degeneration observed in the *mafG*$^{-/-}$::*mafK*$^{+/-}$ mutant mice might have a common link to other neurodegenerative disorders. Therefore we assessed these same tissue sections for the presence of apoptotic neurons, whose presence is a common consequence of neurodegenerative diseases (21). We observed that neurons in the CA3 region of the hippocampus as well as several thalamic neurons were lost due to apoptosis by 6 weeks of age. Importantly however, we failed to detect a diminished number of neurons in the rest of the CNS, such as in the brain stem or spinal cord (data not shown). Consistent with these observations, neuronal loss was no more apparent in 30-week-old mutants than in the 10-week-old mutants. Thus the progressive and dosage-dependent defect in the small *maf* gene mutant mice differs from most neurodegenerative disorders in that, although the neurons display many cytopathological hallmarks of functional impairment, these are not accompanied by neuronal cell death.

Diminished expression of glycine receptor α 1 receptor in small *maf* gene mutant mice. We next addressed how the neurocytological abnormalities detected in the *mafG*$^{-/-}$::*mafK*$^{+/-}$ mutants might lead to the abnormal startle response since this was the single most prominent phenotype of these mutant mice. In surveying the literature describing phenotypes similar to those described here, we found several reports describing natural mouse mutants that display an abnormal response to startle stimuli, including mutations in the α (18, 30) and β subunit (17) genes of the murine inhibitory glycine receptors. Each of these *Glr* mutants displays long-lasting myoclonus and exaggerated startle responses. Glycine is a major inhibitory neurotransmitter in the spinal cord and brain stem, where its receptor is most abundant. Since neuronal degeneration was most prominent in the spinal cords and brain stems of these *mafG*$^{-/-}$::*mafK*$^{+/-}$ mutant mice, we conjectured that defective glycine receptor expression might account for at least a subset of the behavioral abnormalities displayed by the *maf* mutant animals.

To test the hypothesis that a small Maf deficiency might lead to diminished expression of inhibitory glycine receptors, we examined the steady *maf* accumulation of glycine receptor subunits in the small-*maf* gene mutant animals by RNA blot analysis. Diminished abundance of the Glra1 transcript in the brain stems of symptomatic mutant mice (Fig. 4A) was confirmed by quantitative analysis (Fig. 4B), although changes in Glrb transcript accumulation in symptomatic mutant mice was not statistically significant. The difference in abundance of mRNA expressed by one of the glutamate receptor genes (*NMDAR1*) between *mafG*$^{+/-}$::*mafK*$^{+/-}$ and *mafG*$^{-/-}$::*mafK*$^{+/-}$ mice was insignificant (Fig. 4A and B), suggesting that *Glra1* transcription was selectively diminished. Thus the reduction in Glra1 mRNA abundance (Fig. 4A) was directly reflective of reduced neuronal receptor abundance (Fig. 4C).

Finally, we examined Glra1 mRNA levels during the course of neonatal development. Since *Glra1* begins to be expressed between 2 and 3 weeks after birth, no expression was observed in newborns (Fig. 4D, lanes 1 to 4). At 3 weeks, *Glra1* expression in the mutant animals was slightly diminished in comparison to controls (Fig. 4D, lanes 5 to 8). However, by 10 weeks of age, Glra1 mRNA accumulation was significantly lower in the mutant CNS (Fig. 4D, lanes 11 and 12) than in the control (Fig. 4D, lanes 9 and 10) CNS. Therefore, *Glra1* reduction coincides with the progress of neuronal degeneration and phenotypic onset.

Small Maf loss in the CNS of affected mice results in selective alteration of MARE-dependent gene expression. Since MafG and MafK exert their function through homo- or heterodimeric binding to MAREs, we suspected that altering the molecular ratios between various large-subunit (CNC and Bach) transcription factors that interact with small Maf proteins might be distorted in *mafG*$^{-/-}$::*mafK*$^{+/-}$ mutant neurons (3, 24, 25). However, since it is not known whether or not *Glra1* is regulated by MARE(s), we examined the influence of altered small Maf abundance on MARE-dependent antioxidant gene regulation in the CNS. We showed previously that a large group of antioxidant-responsive genes are regulated through MAREs (10, 12), and, since an impaired defense mechanism against oxidative stress is regarded as a possible cause of neurodegeneration (1), we examined the expression of four well-characterized MARE-dependent oxidative stress-responsive genes in the *maf* mutants: genes encoding NAD(P)H quinone oxidoreductase (NQO1), MSP23 (also called peroxiredoxin I), glutathione *S*-transferase subunit Pi (GST-Pi), and heme oxygenase 1 (HO-1) (10). We found that *HO-1* gene expression was dramatically induced in 10-week-old *mafG*$^{-/-}$::*mafK*$^{+/-}$ mutant brains in comparison to *mafG*$^{+/-}$::*mafK*$^{+/-}$ control brains: *HO-1* induction was observed in the cerebrum, cerebellum, brain stem, and spinal cord (Fig. 5A, top). In surprising contrast, very little change in *GST-Pi* (Fig. 5A, middle) or *NQO1* or *MSP23* (data not shown) was detected.

To identify the cells expressing the most abundant HO-1 mRNA, we performed in situ hybridization analysis on brain stem sections. Strong staining was observed in neurons of *mafG*$^{-/-}$::*mafK*$^{+/-}$ mutant brains (Fig. 5B), but no staining

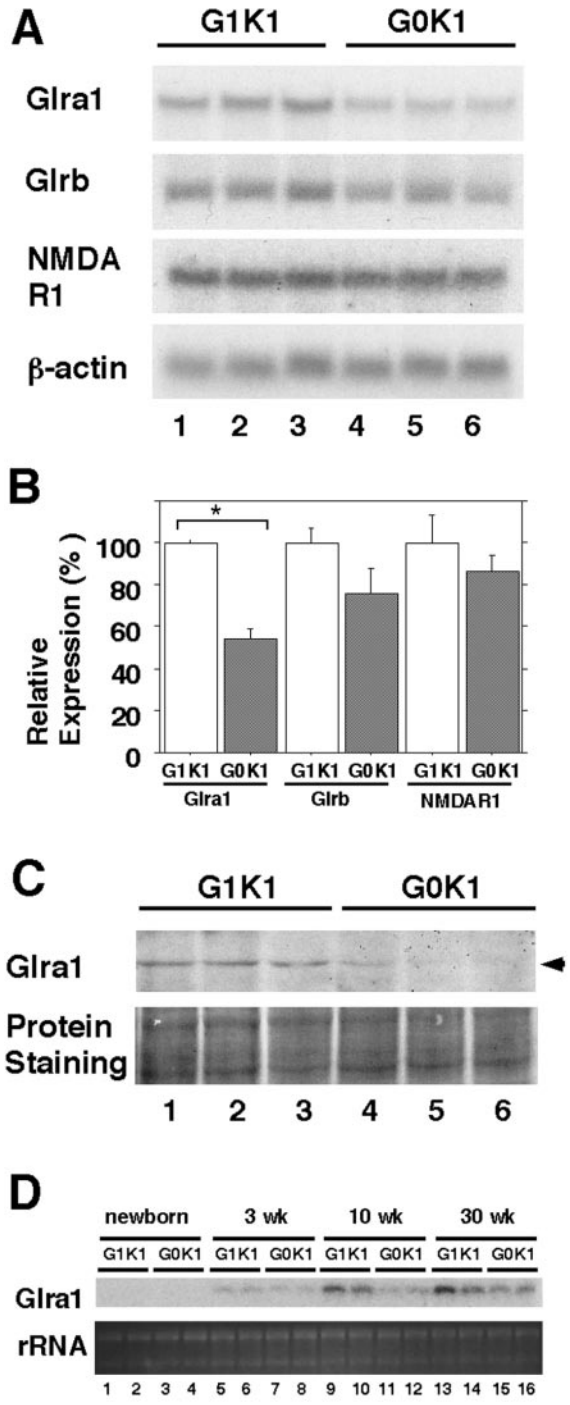

FIG. 4. Expression of glycine receptor α1 and β subunits in the CNS of small *maf* gene compound mutant mice. (A) RNA samples prepared from individual *mafG*$^{+/-}$::*mafK*$^{+/-}$ control mice (lanes 1 to 3) or *mafG*$^{-/-}$::*mafK*$^{+/-}$ mutant mice (lanes 4 to 6) were hybridized to probes corresponding to the *Glra1*, *Glrb*, or *NMDAR1* genes; these were normalized to β-actin expression as the internal control. (B) The data shown in panel A were quantified on a phosphorimager and then normalized to the internal control. *, $P < 0.05$. (C) The abundance of a Glra1 receptor subunit was examined by immunoblotting using an anti-α1 subunit antibody. Protein samples were prepared from individual *mafG*$^{+/-}$::*mafK*$^{+/-}$ control mice (lanes 1 to 3) and *mafG*$^{-/-}$::*mafK*$^{+/-}$ mutant mice (lanes 4 to 6). Protein staining was used to confirm equivalent protein loading. G0K1 and G1K1 are as defined for Fig. 1. (D) *Glra1* reduction was examined by RNA blot analysis using RNA samples prepared from the CNS of individual newborn mice (lanes 1 to 4) or animals 3 (lanes 5 to 8), 10 (lanes 9 to 12), or 30 weeks of age (lanes 13 to 16). RNA samples from *mafG*$^{+/-}$::*mafK*$^{+/-}$ control (lanes 1, 2, 5, 6, 9, 10, 13, and 14) and *mafG*$^{-/-}$::*mafK*$^{+/-}$ mutant littermates (lanes 3, 4, 7, 8, 11, 12, 15, and 16) were examined.

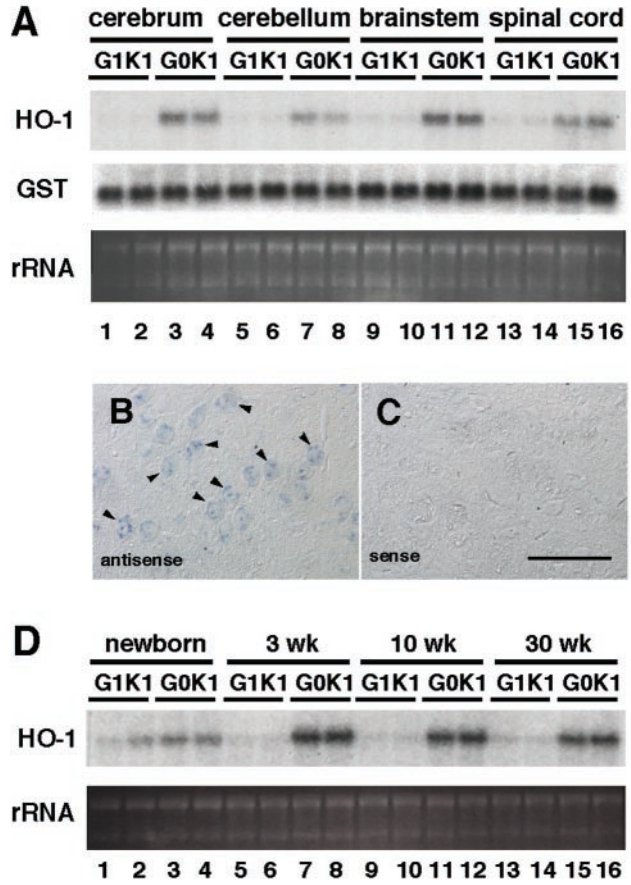

FIG. 5. HO-1 is induced in the *mafG*$^{-/-}$::*mafK*$^{+/-}$ mutant CNS. (A) RNA blot analysis was performed to examine the expression of *HO-1* and *GST-Pi* by using RNA samples prepared from the cerebrums (lanes 1 to 4), cerebellums (lanes 5 to 8), brain stems (lanes 9 to 12), and spinal cords (lanes 13 to 16) of individual 10-week-old *mafG*$^{+/-}$::*mafK*$^{+/-}$ control mice (lanes 1, 2, 5, 6, 9, 10, 13, and 14) and *mafG*$^{-/-}$::*mafK*$^{+/-}$ mutant mice (lanes 3, 4, 7, 8, 11, 12, 15, and 16). G0K1 and G1K1 are as defined for Fig. 1. (B and C) In situ hybridization was performed to examine the distribution of *HO-1*-expressing cells in the *mafG*$^{-/-}$::*mafK*$^{+/-}$ mutant brain stems at 5 weeks of age. Arrowheads, positively stained neurons. Scale bar (C), 60 μm. (D) *HO-1* induction was examined by RNA blot analysis using RNA samples prepared from the CNS of individual newborn mice (lanes 1 to 4) and animals 3 (lanes 5 to 8), 10 (lanes 9 to 12), or 30 weeks of age (lanes 13 to 16). RNA samples from *mafG*$^{+/-}$::*mafK*$^{+/-}$ controls (lanes 1, 2, 5, 6, 9, 10, 13, and 14) and *mafG*$^{-/-}$::*mafK*$^{+/-}$ mutant littermates (lanes 3, 4, 7, 8, 11, 12, 15, and 16) were examined.

above background was observed in neurons of the *mafG*$^{+/-}$::*mafK*$^{+/-}$ controls (data not shown). Hence, selective *HO-1* induction is observed only in CNS neurons of the affected *mafG*$^{-/-}$::*mafK*$^{+/-}$ mutant animals.

We then examined HO-1 mRNA levels during the course of neonatal development. In newborns, where no morphological

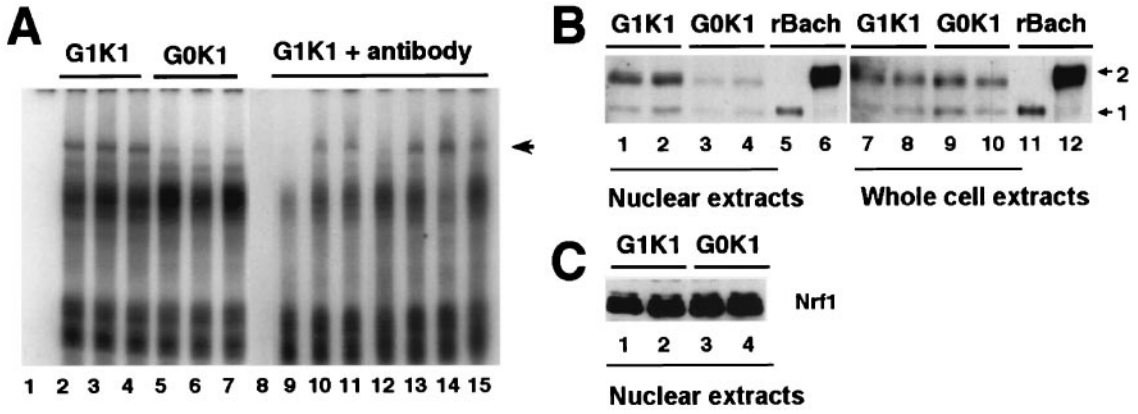

FIG. 6. MARE-binding activity of the Bach/small Maf heterodimer is reduced due to inhibition of Bach nuclear localization in the *maf* mutant mouse brain. (A) EMSA was performed with a probe containing a consensus MARE (see Materials and Methods). The probe was incubated without added nuclear extract (lanes 1 and 8) or with nuclear extract prepared from *mafG*$^{+/-}$::*mafK*$^{+/-}$ control mouse brains (lanes 2 to 4 and 9 to 15) and *mafG*$^{-/-}$::*mafK*$^{+/-}$ mutant mouse brains (lanes 5 to 7). The intensity of the lowest-mobility complex (arrow) was reduced in the mutant brains (lanes 5 to 7). Formation of this complex was inhibited by preincubation of extracts with an anti-small Maf antibody (lane 9) or an anti-Bach antibody (lane 12) but not with anti-p45 NF-E2, anti-Nrf1, anti-Fos, anti-Jun, or preimmune antibodies (lanes 10, 11, 13, 14, and 15, respectively). G0K1 and G1K1 are as defined for Fig. 1. (B and C) Nuclear extracts (lanes 1 to 4) and whole-cell extracts (lanes 7 to 10) were prepared from control *mafG*$^{+/-}$::*mafK*$^{+/-}$ mouse brains (lanes 1, 2, 7, and 8) or *mafG*$^{-/-}$::*mafK*$^{+/-}$ mutant mouse brains (lanes 3, 4, 9, and 10). Recombinant Bach1 and Bach2 proteins served as the positive control (rBach; lanes 5, 6, 11, and 12). Anti-Bach (B) and anti-Nrf1 (C) antibodies were used for immunoblot analysis. Arrows 1 and 2, mobilities of Bach1 and Bach2, respectively.

or phenotypic changes are yet apparent in the *maf* mutant brain, *HO-1* expression was slightly elevated in comparison to controls (Fig. 5D, lanes 1 to 4). However, after 3 weeks of age, the earliest detectable time of any neuropathology in these mice, HO-1 mRNA accumulation was significantly higher in the mutant (Fig. 5D, lanes 7 and 8) than in the control CNS (Fig. 5D, lanes 5 and 6), and this differential expression persisted into adulthood (Fig. 5D, lanes 9 to 16). Therefore, *HO-1* induction preceded the onset of any morphological changes in affected CNS neurons and became prominent coincident with the time of progressing neuronal degeneration and phenotypic onset. These results strongly suggested that the disturbance of MARE-dependent transcriptional regulation was responsible for the failure to maintain normal CNS function in the *maf* mutant mice.

Bach/small Maf heterodimers are reduced in abundance in the *maf* mutant CNS. We next examined MARE-dependent binding activities in *mafG*$^{-/-}$::*mafK*$^{+/-}$ brain extracts. We performed EMSA using a consensus MARE sequence as the probe (see Materials and Methods). Using nuclear extracts prepared from compound heterozygous mutant (control) brains, we found that several proteins formed complexes with the MARE (Fig. 6A, lanes 2 to 4). When equivalent samples from the *mafG*$^{-/-}$::*mafK*$^{+/-}$ mutant mice were examined in kind, only the lowest-mobility band was significantly altered in intensity (Fig. 6A, lanes 5 to 7). This complex was specifically inhibited by the addition of an excess of an unlabeled MARE-containing oligonucleotide but not by a scrambled oligonucleotide (data not shown), indicating that this binding activity was specific for the MARE sequence.

When an antibody against the small Maf proteins was included in the EMSA reaction, most of the complexes (including the entire lowest-mobility band) diminished in intensity (Fig. 6A, lane 9), demonstrating that small Mafs participate in these complexes. Addition of an antibody that recognizes both Bach proteins (29) interfered with formation of the lowest-mobility complex (Fig. 6A, lane 12). In contrast, this same complex was unaltered when antibodies recognizing p45 NF-E2, Nrf1, c-Jun, or c-Fos were preincubated with the extracts (Fig. 6A, lanes 10, 11, 13, and 14, respectively). These data indicated that the electrophoretically distinct lowest-mobility complex contained both small Maf and Bach proteins and was significantly less abundant in the *mafG*$^{-/-}$::*mafK*$^{+/-}$ mutant than in the control brain. We tentatively concluded that the reduction in abundance of Bach/small Maf heterodimers in the mutants might represent a key biochemical deficiency, thus altering the normal transcription of genes regulated by MAREs in the CNS of the *mafG*$^{-/-}$::*mafK*$^{+/-}$ mutant mice.

Suppression of Bach protein nuclear localization in small *maf* gene mutant brains. To test the hypothesis that diminished Bach/small Maf complex formation might be attributable to reduced small Maf abundance in the mutant CNS, we next asked whether or not the abundance of Bach proteins in the mutants was altered (since Bach homodimers cannot bind to MAREs [29]). To this end, we compared nuclear extracts prepared from the brains of mutant and control mice by immunoblotting using an anti-Bach antibody. The levels of both Bach1 and Bach2 were significantly reduced in *mafG*$^{-/-}$::*mafK*$^{+/-}$ mutant brain nuclear extracts compared to those in *mafG*$^{+/-}$::*mafK*$^{+/-}$ controls (Fig. 6B, lanes 1 to 6), while the abundance of another CNC family protein, Nrf1, in mice with the two genotypes was unchanged (Fig. 6C). When we repeated the immunoblot analysis with whole-cell extracts instead of nuclear extracts, we were surprised to find that there was no difference in Bach protein abundance between the two samples (Fig. 6B, lanes 7 to 12). We tentatively concluded that the Bach proteins, normally found exclusively in the nucleus, reside predominantly in the cytoplasm in the neurons of *mafG*$^{-/-}$::*mafK*$^{+/-}$ mutant mice. If true, this conclusion also implied that stable nuclear accumulation of the Bach proteins

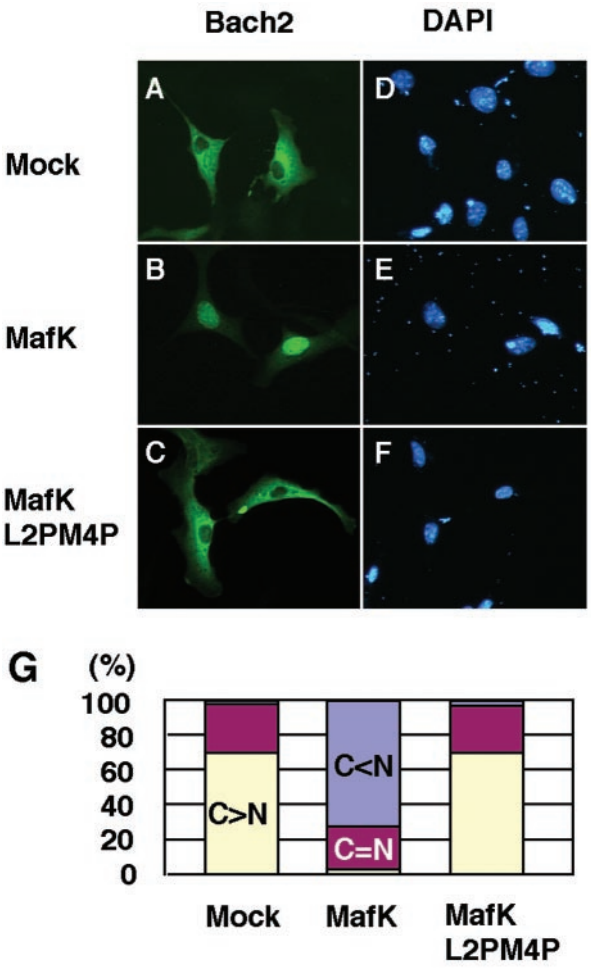

FIG. 7. Small Maf proteins promote nuclear localization of Bach2. NIH 3T3 cells were examined for subcellular localization of transfected Bach2 protein (A to C) or location of nuclei in these cells using DAPI (D to F). The Bach2 expression plasmid was either transfected alone (A and D) or cotransfected with a vector directing expression of *mafK* (B and E) or a *mafK* mutant in two positions that disrupts dimerization (MafKL2PM4P; C and F). (G) Quantitative analysis of subcellular localization of Bach2. A total of 100 transfected cells were examined for Bach2 localization and classified into three different categories: C>N, predominantly cytoplasmic; C=N, equally distributed; C<N, predominantly nuclear.

depends directly on the availability and/or abundance of small Maf proteins.

Small Maf proteins promote nuclear localization of Bach proteins. To test the hypothesis that small Maf proteins can affect the subcellular distribution of Bach factors, Bach2 was transiently expressed in NIH 3T3 cells and its subcellular localization was determined by indirect immunofluorescence using the anti-Bach antibody. When Bach2 alone was transfected, immunostaining was observed exclusively in the cytoplasm as previously reported (Fig. 7A and D) (7). In contrast, when Bach2 was transfected with MafK, Bach2 accumulated predominantly within nuclei (Fig. 7B and E). The same result was observed when Bach2 and MafG were coexpressed (not shown), while coexpression of Bach2 with the MafK leucine zipper mutant, MafKL2PM4P (23), which fails to heterodimerize with Bach or CNC proteins, failed to promote Bach2 nuclear localization (Fig. 7C and F). When Bach1 was transfected instead of Bach2, MafG and MafK had effects identical to those that they had on Bach2 cellular localization (data not shown). Taken together, these results demonstrate that the small Maf proteins promote translocalization of Bach1 and Bach2 from the cytoplasm into the nucleus and that the leucine zipper motif of the small Mafs is essential for this function. These results suggested an intriguing possibility for a novel function of the small Maf proteins in transcriptional regulation: besides being required for binding site specificity for the MARE (extended AP-1) sequence (25), they may promote preferred nuclear localization of heterodimeric partner subunits (CNC and Bach family members) that are required for transcriptional activation and repression.

DISCUSSION

In this study, we focused on a progressive neurological disorder that we first detected in *mafG* homozygous mutant mice (31) and that was quite dramatically exacerbated in *mafG*::*mafK* compound mutant animals (28). While the neurological symptoms in *mafG*$^{-/-}$ mice were detectable in only a fraction of the mutant animals and only after they reached 25 weeks or more of age, a more extreme version of essentially the same neuropathology was fully developed by 9 weeks of age in *mafG*$^{-/-}$::*mafK*$^{+/-}$ mice with >90% penetrance. One characteristic of this neuropathology was intermittent and long-lasting myoclonus, which could be triggered by external or internal stimuli. This phenotype immediately suggested that neuronal excitability was abnormally facilitated or that inhibitory inputs to neuromotor function were defective.

Since we found that the *maf* mutants displayed abnormal startle responses that could be triggered by acoustic stimuli, we searched for natural mutants that were reported to have similar characteristics. The example of natural mutant mice with defective glycine receptor subunit genes (*Glra1 and Glrb*) was most intriguing (17, 18, 30). Glycine is a major inhibitory neurotransmitter after birth, affecting transmission in the spinal cord and brain stem. The glycine postsynaptic receptor consists of ligand-binding α and structural β subunits, which assemble to form a glycine-gated chloride channel. Mice homozygous for *oscillator* (*spd*^{ot}), a null mutation in the *Glra1* gene, develop severe tremors and die by 3 weeks of age, while heterozygous *oscillator* animals display no abnormal behavior but have an increased acoustic startle response, conferred by a haploinsufficiency in glycine receptor function (18). We therefore suspected that aspects of the phenotype observed in *mafG*$^{-/-}$::*mafK*$^{+/-}$ mice might be caused by diminished glycine receptor expression.

As anticipated, we found reduced glycine receptor expression in the CNS of *mafG*$^{-/-}$::*mafK*$^{+/-}$ mice. The phenotype observed in these mutant mice was more severe than that observed in heterozygous *spd*^{ot} mice but milder than that observed in the homozygous mutant animals. This intermediate phenotype may indicate that α 1 receptor expression in *mafG*$^{-/-}$::*mafK*$^{+/-}$ mice is severely reduced but not completely eliminated. Diminished β subunit expression may also contribute to the symptoms of *mafG*$^{-/-}$::*mafK*$^{+/-}$ mice, although we were unable to document a statistically significant

difference in *Glrb* abundance. In this regard, it has been shown that *Glrb* transgene-complemented *spastic* mice that retain 25% of wild-type Glr activity display little phenotype (2), suggesting that the twofold Glr reduction exhibited in the *mafG*$^{-/-}$::*mafK*$^{+/-}$ mutants must be at most only partially responsible for the complex neuromotor disturbance reported here.

Reduced glycine receptor accumulation in the *maf* mutants could be a direct consequence of small Maf deficiency or a reflection of protein aggregation in neuronal nuclei that indirectly interferes with cellular processes that ultimately impair the functionality of these proteins. Since very little is known about the transcriptional regulatory mechanisms controlling *Glra1* and *Glrb*, we cannot distinguish between these possibilities at present (attempts to identify MAREs in the two promoters by simple sequence searches failed to reveal genuine small Maf regulatory target sites). It should be noted that neurological signs observed in *mafG*$^{-/-}$::*mafK*$^{+/-}$ mice did not completely overlap with those in the natural glycine receptor mutants. In particular, affected neurons are distributed throughout the CNS, not only in the spinal cords and brain stems, of *mafG*$^{-/-}$::*mafK*$^{+/-}$ mice. However, we found that the CA3 region of the hippocampus and a part of the thalamus both suffer almost complete cellular loss from apoptosis in the mutant, but not in the control, animals (data not shown). Thus lesions in other regions of the brain may be responsible for additional neurological abnormalities that lead to complex phenotypes in these mice that we have not yet deciphered. To better understand the molecular origins of the compound *maf* mutant phenotypes, we are in the process of detailed comparisons to several mouse neurological mutations (*oscillator*, *stargazer*, *spasmodic*, and *spastic*) (2, 17, 18, 30) whose phenotypes each display overlapping similarities to the phenotypes reported here.

Histological examination of the small *maf* gene compound mutants revealed that neurons in the spinal cord, brain stem, and other parts of the CNS became chromatolytic and that ubiquitinated protein aggregates increased in the nuclei of these affected neurons. Accumulation of aggregated proteins is frequently observed in neurodegenerative diseases (1), and three major factors have been proposed for the formation of inclusion bodies or extracellular aggregates: one is that a mutated gene product itself aggregates, a second is that proteins become oxidized and denatured due to oxidative stress, and a third is that protein degradation mechanisms are somehow rendered defective. In the *mafG*$^{-/-}$::*mafK*$^{+/-}$ mutant mice, we anticipated that general neuronal defense mechanisms against oxidative stress might be impaired since most antioxidant-responsive genes are regulated through MARE sequences (11, 24). To our surprise, however, we detected changes in the expression of only one of the four antioxidant genes examined, *HO-1* (see below). We concluded from these data that cytological changes in neurons of the *mafG*$^{-/-}$::*mafK*$^{+/-}$ mutant mice share some, but not all, of the characteristics that are often found in human neurodegenerative disorders. Although we first anticipated that reduced expression of MARE-dependent genes in neurons might lead to neuronal degeneration, all of the MARE-dependent target genes we examined were unchanged except for *HO-1*, and there was no apparent age-dependent reduction in the number of neurons through either cell death or apoptosis. Unexpectedly, *HO-1* was markedly induced, coincident with a clear reduction in the Bach/small Maf EMSA complex, in brain nuclear extracts prepared from the *mafG*$^{-/-}$::*mafK*$^{+/-}$ mutant mice. Since Bach proteins are expressed in neurons (29), as are MafK and MafG (25) (Fig. 2), Bach/small Maf heterodimers were predicted to exist in neuronal cells. Bach family proteins are reported to be transcriptional repressors (29), and thus any reduction in the amount of Bach/small Maf heterodimers would be expected to lead to relief of repression (induction) of Bach/small Maf-regulated MARE-dependent genes. Recently, we reported that Bach1 null mutant mice also exhibit increased HO-1 mRNA accumulation (34). In that report, we performed chromatin immunoprecipitation assays to demonstrate that small Maf proteins bind to the functional MARE sequence located in the *HO-1* regulatory sequences (34). *HO-1* induction in the *maf* mutant mice serves as clear complementary evidence for disturbance of this MARE-dependent regulatory event. While increased *HO-1* gene expression might contribute to increased cytotoxicity (35), abundant HO-1 itself may not be an underlying cause for the observed neuronal deterioration in the *maf* mutants, since HO-1 also plays a role in cytoprotection against oxidative stress (35). Dysregulation of some currently unidentified MARE-dependent gene(s) (encoding glycine receptor subunits, proteasome components, or other factors in this circuitry) may be the primary pathogenic event.

Although diminished expression of Bach/small Maf heterodimers was the most readily apparent alteration in the EMSA pattern of *maf* mutant brain extracts, we cannot overlook the far more abundant contribution of CNC regulatory proteins that partner with small Mafs (Nrf1, Nrf2, and Nrf3) to regulate transcription through MAREs (e.g., the most abundant gel shift product in Fig. 6A), since all of these CNC family members are also expressed in the brain. The antiserum against the small Maf proteins reacts not only with the low-mobility Bach/small Maf heterodimer but also with all the other more abundant complexes (Fig. 6A, lane 9). Since the intensity of this broad, higher-mobility band in the *mafG*$^{-/-}$::*mafK*$^{+/-}$ brain extracts was essentially the same as that in control extracts, one initial assumption might be that the corresponding binding activities in the mutant extracts may be unchanged. However, since the tissue extracts are not purely neuronal, contributions from glia might mask even quite significant neuronal depletion of any of the CNC proteins. If this were the case, then altered neuronal composition of the higher-mobility band could also be a contributing factor to the observed neuronal deterioration. To address the question of which MARE-interacting proteins are directly responsible for the motor disorder, we would need to know the detailed consequences of mutations in each of these *CNC* genes in the CNS, but, to date, germ line mutation of the *CNC* genes has failed to display neurological phenotypes (5, 11, 32, 33).

We showed that small Maf proteins facilitated nuclear localization of Bach proteins in vivo and in vitro, revealing another novel aspect of small Maf function in transcriptional regulation. Bach1 and Bach2 both have nuclear and cytoplasmic localization signals (NLS and CLS, respectively) (7), and Bach2 nuclear localization is regulated by the cellular nuclear export system through its CLS in response to stimuli such as oxidative stress (7). It was also reported that Bach1t, which lacks a CLS, confers a preferred nuclear localization to Bach1,

and the hypothesis that subcellular localization of Bach is determined by the net balance between NLS and CLS activity was proposed (13). This hypothesis can now be extended if we incorporate the properties of the Bach/small Maf complex described here. We showed that, under normal conditions, the Bach proteins, possessing one CLS and one NLS, are preferentially localized in the cytoplasmic compartment (presumably because of greater CLS activity or lesser NLS activity). After Bach proteins heterodimerize with small Mafs, which possess only an NLS, the two proteins together now bear two NLS and one CLS. We infer that the two-to-one ratio between NLS and CLS activities within this heterodimeric complex may be required for stable nuclear accumulation of Bach proteins. Since MafKL2PM4P, a leucine zipper MafK mutant, was unable to facilitate nuclear import of Bach, we conclude that heterodimerization between Bach and small Maf proteins is essential for the nuclear confinement of Bach proteins, supporting this NLS-CLS "balance" hypothesis.

This study provides the first insights detailing the significance of MARE-dependent transcriptional regulation in the execution of normal CNS function. In this work, we chose to examine *mafG*$^{-/-}$::*mafK*$^{+/-}$ mice for the analysis of a specific neurological disorder. Although this severe motor phenotype is fully penetrant in *mafG*$^{-/-}$::*mafK*$^{+/-}$ mice, the mice still have an almost-normal life span. When an even greater number of defective small *maf* alleles are introduced into this background, the effect is lethal, either before weaning or in utero (28; F. Katsuoka and H. Motohashi, unpublished data). The degree of small Maf reduction in the *mafG*$^{-/-}$::*mafK*$^{+/-}$ mutant mice was optimal for generating the neuropathology we wished to analyze. Thus one important conclusion of this work is that hypomorphic mutants, created by combining lesions in multiple genes that are likely to be compensatory may serve as a powerful tool for analyzing the pathogenesis of adult human diseases, since these experimental animals exhibit specifically impaired cellular functions and yet survive.

ACKNOWLEDGMENTS

We are grateful to Kim-Chew Lim and M. Masu for critical discussions and advice. We thank T. Ishii for providing the HO-1 cDNA and S. Nakanishi for providing the NMDAR1 cDNA. We also thank N. Kaneko for technical support in histological analysis and R. Kawai for mouse breeding.

This work was supported by NIH grant CA80088 to J.D.E., grants from the Ministry of Education, Culture, Sports, Science and Technology (H.M. and M.Y.), JSPS-RFTF, and CREST (M.Y.), and the Special Coordination Fund for Promoting Science and Technology and PROBRAIN (H.M.).

REFERENCES

1. **Alves-Rodrigues, A., L. Gregori, and M. E. Figueiredo-Pereira.** 1998. Ubiquitin, cellular inclusions and their role in neurodegeneration. Trends Neurosci. **21:**516–520.
2. **Becker, L., B. Hartenstein, J. Schenkel, J. Kuhse, H. Betz, and H. Weiher.** 2000. Transient neuromotor phenotype in transgenic spastic mice expressing low levels of glycine receptor beta-subunit: an animal model of startle disease. Eur. J. Neurosci. **12:**27–32.
3. **Blank, V., and N. C. Andrews.** 1997. The Maf transcription factors: regulators of differentiation. Trends Biochem. Sci. **22:**437–441.
4. **Dignam, J. D.** 1990. Preparation of extracts from higher eukaryotes. Methods Enzymol. **182:**194–203.
5. **Farmer, S. C., C.-W. Sun, G. E. Winnier, B. L. M. Hogan, and T. M. Townes.** 1997. The bZip transcription factor LCR-F1 is essential for mesoderm formation in mouse development. Genes Dev. **11:**786–798.
6. **Fukamauchi, F., N. Mataga, Y. J. Wang, S. Sato, A. Youshiki, and M. Kusakabe.** 1996. Abnormal behavior and neurotransmissions of tenascin gene knockout mouse. Biochem. Biophys. Res. Commun. **221:**151–156.
7. **Hoshino, H., A. Kobayashi, M. Yoshida, N. Kudo, T. Oyake, H. Motohashi, N. Hayashi, M. Yamamoto, and K. Igarashi.** 2000. Oxidative stress abolishes leptomycin B-sensitive nuclear export of transcription repressor Bach2 that counteracts activation of Maf recognition element. J. Biol. Chem. **275:**15370–15376.
8. **Igarashi, K., K. Itoh, N. Hayashi, M. Nishizawa, and M. Yamamoto.** 1995. Conditional expression of the ubiquitous transcription factor MafK induces erythroleukemia cell differentiation. Proc. Natl. Acad. Sci. USA **92:**7445–7449.
9. **Igarashi, K., K. Itoh, H. Motohashi, N. Hayashi, Y. Matuzaki, H. Nakauchi, M. Nishizawa, and M. Yamamoto.** 1995. Activity and expression of murine small Maf family protein MafK. J. Biol. Chem. **270:**7615–7624.
10. **Ishii, T., K. Itoh, S. Takahashi, H. Sato, T. Yanagawa, Y. Katoh, S. Bannai, and M. Yamamoto.** 2000. Transcription factor Nrf2 coordinately regulates a group of oxidative stress-inducible genes in macrophages. J. Biol. Chem. **275:**16023–16029.
11. **Itoh, K., T. Chiba, S. Takahashi, T. Ishii, K. Igarashi, Y. Katoh, T. Oyake, N. Hayashi, K. Satoh, I. Hatayama, M. Yamamoto, and Y. Nabeshima.** 1997. An Nrf2/small Maf heterodimer mediates the induction of phase II detoxifying enzyme genes through antioxidant response elements. Biochem. Biophys. Res. Commun. **236:**313–322.
12. **Itoh, K., T. Ishii, N. Wakabayashi, and M. Yamamoto.** 1999. Regulatory mechanisms of cellular response to oxidative stress. Free Radic. Res. **31:**319–324.
13. **Kanezaki, R., T. Toki, M. Yokoyama, K. Yomogida, K. Sugiyama, M. Yamamoto, K. Igarashi, and E. Ito.** 2001. Transcription factor BACH1 is recruited to the nucleus by its novel alternative spliced isoform. J. Biol. Chem. **276:**7278–7284.
14. **Kataoka, K., K. Igarashi, K. Itoh, K. T. Fujiwara, M. Noda, M. Yamamoto, and M. Nishizawa.** 1995. Small Maf proteins heterodimerize with Fos and may act as competitive repressors of the NF-E2 transcription factor. Mol. Cell. Biol. **15:**2180–2190.
15. **Katsuoka, F., H. Motohashi, K. Onodera, N. Suwabe, J. D. Engel, and M. Yamamoto.** 2000. One enhancer mediates *mafK* transcriptional activation in both hematopoietic and cardiac muscle cells. EMBO J. **19:**2980–2991.
16. **Kawai, S., N. Goto, K. Kataoka, T. Saegusa, H. Shinno-Kohno, and M. Nishizawa.** 1992. Isolation of the avian transforming retrovirus, AS42, carrying the *v-maf* oncogene and initial characterization of its gene product. Virology **188:**778–784.
17. **Kingsmore, S. F., B. Giros, D. Suh, M. Bieniarz, M. G. Caron, and M. F. Seldin.** 1994. Glycine receptor β-subunit gene mutation in spastic mouse associated with LINE-1 element insertion. Nat. Genet. **7:**136–141.
18. **Kling, C., M. Koch, B. Saul, and C. M. Becker.** 1997. The frameshift mutation oscillator *Glra1*$^{spd\text{-}ot}$ produces a complete loss of glycine receptor α 1-polypeptide in mouse central nervous system. Neuroscience **78:**411–417.
19. **Kotkow, K. J., and S. H. Orkin.** 1996. Complexity of the erythroid transcription factor NF-E2 as revealed by gene targeting of the mouse p18 NF-E2 locus. Proc. Natl. Acad. Sci. USA **93:**3514–3518.
20. **Masuo, Y., Y. Matsumoto, S. Morita, and J. Noguchi.** 1997. A novel method for counting spontaneous motor activity in the rat. Brain Res. Brain Res. Protoc. **1:**321–326.
21. **Mattson, M. P.** 2000. Apoptosis in neurodegenerative disorders. Nat. Rev. Mol. Cell Biol. **1:**120–129.
22. **Motohashi, H., K. Igarashi, K. Onodera, S. Takahashi, H. Ohtani, M. Nakafuku, M. Nishizawa, J. D. Engel, and M. Yamamoto.** 1996. Mesodermal- vs neuronal-specific expression of MafK is elicited by different promoters. Genes Cells **1:**223–238.
23. **Motohashi, H., F. Katsuoka, J. A. Shavit, J. D. Engel, and M. Yamamoto.** 2000. Positive or negative MARE-dependent transcriptional regulation is determined by the abundance of small Maf proteins. Cell **103:**865–875.
24. **Motohashi, H., T. O'Connor, F. Katsuoka, J. D. Engel, and M. Yamamoto.** 2002. Integration and diversity of the regulatory network composed of Maf and CNC families of transcription factors. Gene **294:**1–12.
25. **Motohashi, H., J. A. Shavit, K. Igarashi, M. Yamamoto, and J. D. Engel.** 1997. The world according to Maf. Nucleic Acids Res. **25:**2953–2959.
26. **Noebels, J. L., X. Qiao, R. T. Bronson, C. Spencer, and M. T. Davisson.** 1990. Stargazer: a new neurological mutant on chromosome 15 in the mouse with prolonged cortical seizures. Epilepsy Res. **7:**129–135.
27. **Onodera, K., J. A. Shavit, H. Motohashi, F. Katsuoka, J. E. Akasaka, J. D. Engel, and M. Yamamoto.** 1999. Characterization of the murine *mafF* gene. J. Biol. Chem. **274:**21162–21169.
28. **Onodera, K., J. A. Shavit, H. Motohashi, M. Yamamoto, and J. D. Engel.** 2000. Perinatal synthetic lethality and hematopoietic defects in compound *mafG::mafK* mutant mice. EMBO J. **19:**1335–1345.
29. **Oyake, T., K. Itoh, H. Motohashi, N. Hayashi, H. Hoshino, M. Nishizawa, M. Yamamoto, and K. Igarashi.** 1996. Bach proteins belong to a novel family of BTB-basic leucine zipper transcription factors that interact with MafK and regulate transcription through the NF-E2 site. Mol. Cell. Biol. **16:**6083–6095.
30. **Ryan, S. G., M. S. Buckwalter, J. W. Lynch, C. A. Handford, L. Segura, R.**

Shiang, J. J. Wasmuth, S. A. Camper, P. Schofield, and P. O'Connell. 1994. A missense mutation in the gene encoding the α 1 subunit of the inhibitory glycine receptor in the spasmodic mouse. Nat. Genet. **7:**131–135.

31. **Shavit, J. A., H. Motohashi, K. Onodera, J. Akasaka, M. Yamamoto, and J. D. Engel.** 1998. Impaired megakaryopoiesis and behavioral defects in *mafG*-null mutant mice. Genes Dev. **12:**2164–2174.
32. **Shivdasani, R. A., and S. H. Orkin.** 1995. Erythropoiesis and globin gene expression in mice lacking the transcription factor NF-E2. Proc. Natl. Acad. Sci. USA **92:**8690–8694.
33. **Shivdasani, R. A., M. F. Rosenblatt, D. Zucker-Franklin, C. W. Jackson, P. Hunt, C. J. Saris, and S. H. Orkin.** 1995. Transcription factor NF-E2 is required for platelet formation independent of the actions of thrombopoietin/MGDF in megakaryocyte development. Cell **81:**695–704.
34. **Sun, J., H. Hoshino, K. Takaku, O. Nakajima, A. Muto, H. Suzuki, S. Tashiro, S. Takahashi, S. Shibahara, J. Alam, M. Taketo, M. Yamamoto, and K. Igarashi.** 2002. Hemoprotein Bach1 regulates enhancer availability of heme oxygenase-1 gene. EMBO J. **21:**5216–5224.
35. **Suttner, D. M., and P. A. Dennery.** 1999. Reversal of HO-1 related cytoprotection with increased expression is due to reactive iron. FASEB J. **13:**1800–1809.